

# Application of Highly Charged Ar Ion Beam to Ion Beam Lithography

Sadao Momota<sup>A</sup>, Yoichi Nojiri<sup>A</sup>, Hisayoshi Hamagawa<sup>A</sup>, Kensuke Hamaguchi<sup>A</sup>, Jun Taniguchi<sup>B</sup>, Hirohisa Ohno<sup>B</sup>  
<sup>A</sup>Kochi University of Technology, Miyano-kuchi, Tosayamada-cho, Kochi, 782-8502, Japan  
<sup>B</sup>Tokyo University of Science, 2641, Yamasaki, Noda, Chiba, 278-8510, Japan



## 1. Introduction

Heavy ion beams are effective tools for the nano-scale modification and fabrication of materials. In ion beam lithography (IBL), a step structure is formed by the change in the etching rate induced by ion beam irradiation. In almost all previous studies on the use of heavy ion beams to IBL, only singly charged ions (SCIs) were utilized. Highly charged ions (HCIs) have several advantages and unique features as revealed by a series of studies. In the present study, highly charged Ar ions were applied to IBL in order to study and confirm the effect of HCI.

## 2. Highly Charged Ions (HCIs)

Unique features of HCIs  
 + Large interaction cross sections  
 + Large potential energy  $\sim q^3$

Phenomena induced by the irradiation of HCIs

+ Coulomb explosion  
 → Potential sputtering  
 ref. Phys. Rev. Lett. 86 (2001) 3530

+ Stopping-power enhancement  
 → Charge state dependent energy loss  
 ref. Phys. Rev. Lett. 79 (1997) 2030

## 3. Experimental setup

General View

1. Production of HCI beam
2. Transport and analysis of HCI beam
3. Irradiation of HCI beam

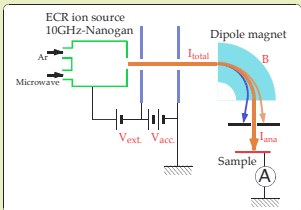


Fig. 1 General view of experimental setup

### 3-1. Production of HCI beam



Fig. 2 Ion source

ECR-ion source 10GHz-NANOGAN (PANTECHNIK Co.)  
 Voltage for beam extraction ( $V_{ext}$ ) : 0 ~ 30 kV  
 Voltage for beam acceleration ( $V_{acc}$ ) : 0 ~ 100 kV  
 Power of RF for ionization ( $P_{RF}$ ) : 0 ~ 80 W

### 3-2. Transport and analysis of HCI beam



Fig. 3 Dipole magnet and irradiation chamber

Transport of ion beams focused by einzel lens and electric Q-lens

Analysis of ion beams  
 A/q analysis by using a dipole magnet  
 $\theta = \pi/2$  [rad]  
 $B\rho = 0 \sim 0.33$  [T-m]

### 3-3. Irradiation of HCI beam

HCI beam was irradiated through a Cu stencil mask.

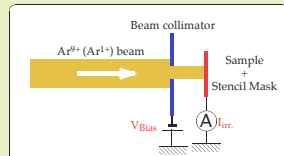


Fig. 4 Schematic view of irradiation system

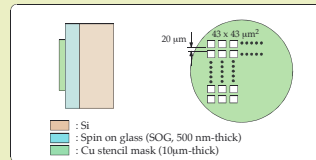


Fig. 5 Sample and stencil mask

## 4. Experimental procedure

1. Preparation of Beam  
 Ion :  $Ar^{9+}$  ( $Ar^{1+}$ )  
 Energy : 90 keV
2. Irradiation of Ar beam  
 100q ~ 500q  $\mu C/cm^2$
3. Chemical etching  
 Etchant : A solution of HF  
 Time : 1 min.
4. Measurements  
 A. Optical micrograph  
 B. Surface profile  
 alpha-step IQ (KLA Tencor Corporation)

## 5. Results

### 5-1. Optical micrograph of SOG

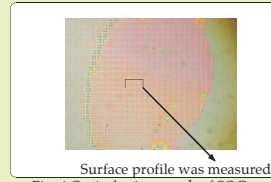


Fig. 6 Optical micrograph of SOG  
 Irradiation :  $Ar^{9+}$ , 400 x 9  $\mu C/cm^2$

The clear transfer of the Cu stencil mask pattern using an  $Ar^{9+}$  and an  $Ar^{1+}$  beam onto the SOG was examined.

### 5-2. Surface profile of SOG

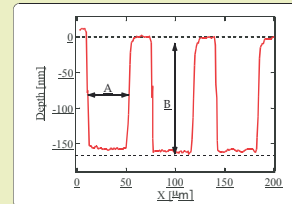


Fig. 7 Surface profile of SOG  
 Irradiation :  $Ar^{9+}$ , 400 x 9  $\mu C/cm^2$

Step structure was fabricated on SOG.

A. Width of hollows at the half depth of maximum	44 ± 1 $\mu m$
Side length of hollows of a Cu stencil mask	Good agreement 43 $\mu m$
B. Depth of step structure	161 ± 1 nm

Define the **etching depth** to be the average depth of a series of three hollows or wells.

### 5-3. Dose and charge state dependence

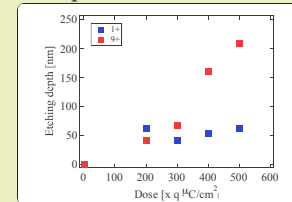


Fig. 8 Etching depth as a function of the Ar ion dose

A. The etching depth with  $Ar^{1+}$  ion was constant as a function of the Ar ion dose over a range of 200 - 500  $\mu C/cm^2$ .

B. The etching depth for  $Ar^{9+}$  ions increased linearly with the Ar ion dose up to 500q  $\mu C/cm^2$ .

C. The etching depth for  $Ar^{9+}$  ions was about 3 times larger than the depth obtained using  $Ar^{1+}$  ions for the dose of 500q  $\mu C/cm^2$ .  
**The HCI effect was observed !!**

## 6. Discussion

6-1. Change in etching rate of SOG  
 The irradiation of  $Ar^{9+}$  ( $Ar^{1+}$ ) ions enhanced the etching rate of SOG using a solution of HF.

6-2. Dose & charge state dependence  
 Etching rate increases with  
 1) the dose of  $Ar^{9+}$  ions → **The HCI effect**  
 2) charge state

Control of etching depth

6-3. Ar-ion induced damage  
 A. Ar-ion induced damage contributing to the etching-rate enhancement extended at least to a depth of ~200 nm from  
 Maximum etching depth = 208 nm ( $Ar^{9+}$ , 500q  $\mu C/cm^2$ )

B. Range (straggling) of Ar ions in  $SiO_2^*$  calculated by SRIM-2003\* : 95 (28) nm (Fig. 7)  
 \*Chemical composition is similar to that of SOG.

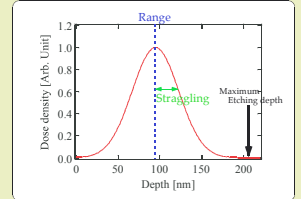


Fig. 9 Range distribution of Ar ions calculated by the SRIM-2003 code

Based on the stopping-power enhancement caused by the HCI effect, the actual range distribution is estimated to be shallower than that derived from the SRIM-2003 calculations

A → Maximum depth of damages contributing to IBL [nm]	> 200
B → Maximum depth of damages created by elastic collisions [nm]	< 100

It is implied that the contribution of the damage caused by **indirect processes** such as mechanical stress and  $\delta$ -electron cascade plays an important role in IBL.

## 7. Conclusion

- $Ar^{9+}$  ions as well as  $Ar^{1+}$  ions were successfully applied to IBL.
- The HCI effect was confirmed as an enhanced etching-rate of SOG.
- The etching depth of SOG can be controlled by the charge state and the dose of the Ar ions.
- The etching depth of SOG, which is larger than the range of Ar ions, suggests that the damage created by indirect processes contributes to the enhancement of etching rate.

In order to more clearly understand the HCI effect, additional systematic studies by varying the charge state and dose are required.